

## Linear optics simulations of the quantum baker's map

John C. Howell and John A. Yeazell

*Department of Physics, The Pennsylvania State University, University Park, Pennsylvania 16802*

(Received 9 July 1999; revised manuscript received 28 September 1999; published 13 December 1999)

The unitary evolution of linear optics can be used to model quantum computational networks. In this paper, a quantum simulation of a classically chaotic map (the baker's map) is developed using linear optics. Two different models are presented. The first model employs only 50-50 beam splitters and phase shifters to simulate universal 2-qubit gates of a quantum computer. The second model uses the discrete Fourier transform generated by symmetric  $N \times N$  fiber couplers. If single photons are used as inputs for these linear optics models, the result is a physical realization of the quantum baker's map.

PACS number(s): 03.67.Lx, 05.45.Mt

### I. INTRODUCTION

Quantum computers have been shown to be superior to classical computers in factoring large numbers [1,2], searching [3,4], and in simulating quantum systems [5]. Several physical systems including ion traps [6], liquid state NMR [7,8], cavity QED [9], far-off-resonance optical lattices [10], and solid state systems [11] have been explored as possible quantum computers. There are only a few requirements for a quantum computer. The quantum bits (qubits) must be strongly entangled with each other. The bits must be easily manipulated by controlled external fields, and minimally coupled to all other fields. For example, the qubits in the ion trap [6] are the ions and these ions are entangled via the Coulomb repulsion. The states of the qubits are the electronic states of the ions, which are manipulated with laser fields.

This paper proposes an all-optical implementation of quantum logic. Many all-optical implementations of quantum logic have been proposed and studied [12–17]. For example, solutions to the factoring problem have been proposed based upon an  $N$ -slit interferometer [14] and upon a simple phase-varying Mach-Zehnder interferometer [15]. Also a linear optics simulation of the Deutsch-Jozsa algorithm has been developed [13]. Of particular interest is the work of Cerf *et al.* [12] and Kwiat *et al.* [17]. They used simple linear optical elements (e.g., 50-50 beam splitters and waveplates) to simulate quantum circuits such as teleportation [18] and an exhaustive search [3,4].

The quantum behavior of linear optics is realized by identifying a particular path with a particular quantum state. For example, a 1-bit simulation requires two paths. The paths are labeled 0 and 1 representing the eigenvectors  $|0\rangle$  and  $|1\rangle$ , respectively. The analogy to the operation of quantum logic gates is particularly apparent in single-photon interferometry experiments. In that case, the quantum bit is directly associated with the “which path” variable [19]. For example, an optical symmetric beam splitter is known to act as the square root of a controlled NOT gate (up to a phase of  $\pi/4$ ) [12]. The key is that a single photon may be used to represent multiple quantum bits.

Typical quantum computers rely heavily on basic 1-bit and 2-bit gates to form the fundamental logic. Hence, algorithms are developed in terms of the most basic gates. This is

true because of the difficulty of implementing more-than-two-bit gates. Therefore, the thrust of many researchers is to show that the 1-bit and 2-bit gates form a complete set of universal gates [20,21]. However, linear optics is not constrained by such limitations. It is only bounded by the physical size of the apparatus [12,22], since the apparatus size grows exponentially with the number of bits. Using linear optics, many  $L$ -bit gates can be implemented in a single unitary operation (a brief discussion is found in [23]).

The discrete Fourier transform (DFT) [2,24] is an example of an operation that can be performed exponentially faster on a quantum computer than on a classical computer. For a typical  $L$ -bit quantum computer, the number of 2-bit operations needed to realize the DFT goes as  $\sum_{l=1}^L l$ . However, for a symmetric multiport [25,26] device, the DFT can be effected in a single unitary operation [27]. This fact will be used to construct a relatively simple quantum baker's map later on in the paper.

Even though it has been shown that linear optics can realize any unitary operation [28] and simulate quantum networks [12], this framework cannot be considered a true quantum computing system. A quantum computer has  $n$ -entangled bits having a  $2^n$ -dimensional Hilbert space. Hence, there are two significant differences. First, in linear optics the entanglement is between different degrees of freedom of a single particle [16]. On the other hand, with typical quantum computing systems many particles are entangled nonlocally. Second, as Barenco *et al.* [22] points out, the physical size of the apparatus performing the computation grows with the number of bits for a quantum computer and with the Hilbert space for a linear optics setup. As Spreuw [16] indicates the exponential growth in the number of paths is a direct consequence of the lack of nonlocality in this system as compared to the typical quantum computer system. In effect then, the result is a classical optical computer, with one exception. If single photons are used, then the results are probabilistic and quantum mechanical. That is, a single implementation of the device using a single photon yields a single realization of the computation. The measurement of the photon will find it in a particular output path. For a weak classical light field input, an ensemble of such individual realizations result. In that case, the output intensities may be associated with the probabilities of finding the photon in a particular output path. In this sense, the implementation of

the computation device with single photons is a quantum analog of the device while the implementation with classical fields is a simulation of the device. However, it should be noted that although it is easy to describe a single photon setup, it is not as easy to experimentally implement one. While great strides have been made in detection [29] and controlled generation of single photons [30], it is still very difficult to work with them. Therefore, we will give examples which utilize classical fields as inputs as well as single photons.

The exponential growth of the linear optical setup with the number of bits poses serious difficulties for implementing a computation device with linear optics. However, linear optics does appear to be a natural framework in which to simulate small- $L$  quantum systems [5,24]. In this case, if a single photon is used as an input then the result is a quantum mechanical realization of the system. If a classical field is used then the result is a simulation of that quantum system.

In this paper, linear optics will be used to model the quantum baker's map (QBM) [24]. Two different setups will be presented. The first setup will simulate the evolution of a typical quantum computer, which uses the basic 2-bit gates. The second, will make use of linear integrated optics which offers some conceptual and possibly technical simplifications.

## II. THE BAKER'S MAP

Simple maps such as the classical baker's map are extremely useful in studying chaotic behavior. They represent a class of completely chaotic systems from which much or all undesirable difficulties, not associated with chaotic behavior, have been removed [31]. By quantizing these classical models, it is hoped that understanding will be gained of how chaotic information is stored in the quantum description of nature and in what limit chaos appears. In addition, simulations have been done on the QBM, which have shown that it is hypersensitive to perturbation of the map [32]. The sensitivity of the QBM to perturbation is a proposed realization of quantum chaos. Schack [24] showed that a simple 3-bit quantum computer could be used to realize the quantum baker's map. It was shown that a sequence of eleven 2-bit gates could realize one iteration of the map. Hannay *et al.* [33] demonstrated one possible optical realization of the quantized baker's map by using the analogy between ray and wave optics and classical and quantum mechanics.

The classical baker's map is a simple area-preserving transformation in the momentum-position phase space. It is assumed that the motion is bounded by  $(Q, P)$ . The motion in phase space [31] is governed by the map

$$(q, p) \mapsto \begin{cases} (2q, \frac{1}{2}p) & \text{if } 0 \leq q < \frac{1}{2}Q, \\ [2q - Q, \frac{1}{2}(p + P)] & \text{if } \frac{1}{2}Q < q \leq Q. \end{cases} \quad (2.1)$$

Hence, the rectangle is compressed to half its original size in the  $p$  dimension and stretched to twice its original size in the  $q$  dimension. Then it is cut in half in the  $q$  dimension and the right most portion is stacked on top of the left most portion.

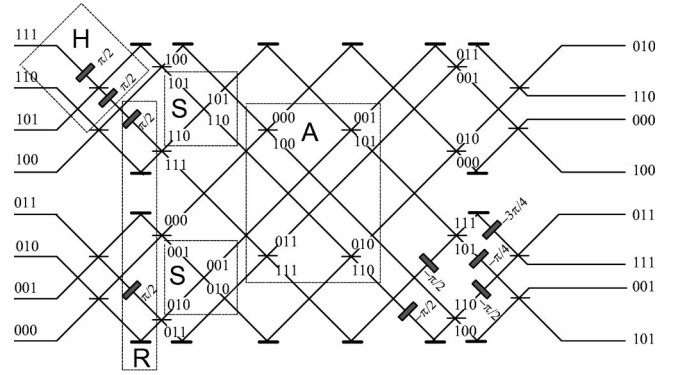


FIG. 1. Optical realization of a 3-bit quantum baker's map using basic 2-bit gates. Transformations ( $R$ ,  $S$ , and  $A$ ) are outlined by dashed boxes. In addition, a 1-bit Hadamard gate is boxed in the upper left-hand corner with a label of  $H$ .

The baker's map is quantized following [31]. The rectangle is divided into phase cells of area  $2\pi\hbar$ . The number of phase cells is given by  $N = PQ/2\pi\hbar$ , where  $PQ$  is an integer multiple of  $2\pi\hbar$ . For three bits, there would be  $2^3 = 8$  cells with a total phase-space area of  $16\pi\hbar$ . Adopting the notation of Balazs and Voros [31], the periodic normalized position eigenvectors are  $|n\rangle$  with eigenvalues  $q_n = 2\pi\hbar n/P$ ,  $n = 0, 1, \dots, N-1$ . The normalized periodic momentum eigenvectors are  $|m\rangle$ , with eigenvalues  $p_m = 2\pi\hbar m/Q$ ,  $m = 0, 1, \dots, N-1$ . The operators  $p$  and  $q$  are defined as translation operators acting on each other's eigenstates. The transformation between the position basis and momentum basis is done by the (DFT) [1,2,24,31] having matrix elements given by

$$(F_N)_{nm} = \langle n|m \rangle = \frac{1}{\sqrt{N}} e^{2\pi i nm/N}. \quad (2.2)$$

The quantum baker's map is defined to be

$$B = F_N^{-1} \begin{pmatrix} F_{N/2} & 0 \\ 0 & F_{N/2} \end{pmatrix}. \quad (2.3)$$

In [2], it is shown that the DFT can be realized by only two basic unitary operations. The first transformation acting on qubit  $j$  is given by

$$A_j = \frac{1}{\sqrt{2}} \begin{pmatrix} 1 & 1 \\ 1 & -1 \end{pmatrix}. \quad (2.4)$$

In [12] this operation is referred to as the Hadamard transformation and was implemented using a beam splitter and two  $-\pi/2$  phase shifters one at each port in the high or 1 path. The transformation can also be considered a 1-bit DFT. Figure 1 has a dashed box around a 1-bit Hadamard gate in the upper left-hand corner. It is important to note that for every beam splitter in the figure there are two phase shifters. The other phase shifters were not drawn for aesthetic reasons.

The second operation is a phase-gate operating on the  $i$ th and  $j$ th ( $i < j$ ) qubits defined by

$$R_{ij}|k_{L-1}, \dots, k_0\rangle = e^{i\varphi_{ij}}|k_{L-1}, \dots, k_0\rangle \quad (2.5)$$

where

$$\varphi_{ij} = \begin{cases} \pi/2^{j-i} & \text{if } k_i = k_j = 1 \\ 0 & \text{otherwise} \end{cases} \quad (2.6)$$

and  $k_m \in \{0,1\}$ . Here,  $L$  is the number of qubits and hence  $N = 2^L$ . The matrix representation of  $R_{ij}$  is given by

$$R_{ij} = \begin{pmatrix} 1 & 0 & 0 & 0 \\ 0 & 1 & 0 & 0 \\ 0 & 0 & 1 & 0 \\ 0 & 0 & 0 & e^{i\varphi_{ij}} \end{pmatrix}. \quad (2.7)$$

The linear optics realization of this gate requires putting a phase delay in the paths where  $i$  and  $j$  are 1. For example, consider a 3-bit circuit. Suppose, the phase gate acts on the zeroth and first bits. Then, the realization of the 3-bit phase gate is to place a  $\pi/2$  phase shift in the 111 and 011 paths as is shown in part  $R$  of Fig. 1 (inside a dashed box labeled  $R$ ).

For  $L$  bits, the total unitary transformation needed to realize the DFT is

$$(A_0 R_{01} \dots R_{0,L-1}) \times \dots \times (A_{L-3} R_{L-3,L-2} R_{L-3,L-1}) \\ \times (A_{L-2} R_{L-2,L-1}) (A_{L-1}) \quad (2.8)$$

It should be noted that (2.8) is not the DFT, unless the qubits are swapped appropriately. Schack [24] used the swap gate  $S_{ij}$ , which swaps qubits  $i$  and  $j$  to obtain the DFT. However, as is pointed out in [24], the swap gate is not needed, if the qubits are relabeled after each execution of Eq. (2.8) or the inverse of Eq. (2.8). When an  $N \times N$  fiber coupler is used to effect the DFT and the inverse DFT, the swap gate is not needed.

Then, for three bits, one iteration of the quantum baker's map [24] is given by

$$B = S_{02} A_0 R_{01}^\dagger R_{02}^\dagger A_1 R_{12}^\dagger A_2 S_{01} A_0 R_{01} A_1. \quad (2.9)$$

The optical realization of this 3-bit transformation is shown in Fig. 1. In Fig. 1, three transformations are boxed in dashed lines and labeled  $R$ ,  $S$ , and  $A$ . These three transformations will be discussed. Since, the other eight transformations are similar to these three transformations, they will not be discussed. Transformation  $R$  is the phase gate  $R_{01}$ . It is realized by placing a phase shift of  $\pi/2$  in paths 111 and 011 (as an aside, all of the path lengths between beam splitters are the same up to the specified phase shifts, even if they are not drawn that way). Transformation  $S$  is the swap gate  $S_{01}$ , which swaps the zeroth and first bit. This is optically realized by crossing and relabeling paths. For example, the 001 and 010 paths cross and are relabeled. Paths such as the 111, where the zeroth and first bit have the same value do not change meaning under the swap gate since they evolve to themselves. Transformation  $A$  is the  $A_2$  operation. Here, all

of the paths are grouped such that the zeroth and first bit are the same upon entering the input ports of the beam splitters. For example, the 000 and 100 enter the top-left-most beam splitter. There are four beam splitters in this transformation accounting for the four possible states of the zeroth and first bit.

To construct Fig. 1 out of free-space optics would be extremely difficult. In order to get pathlengths to subwavelength accuracy for 20 beam splitters would be nontrivial at the very least. However, this simulation is instructive in that it models the operation of a typical 3-bit quantum computer. In addition, for single photons, Fig. 1 is, as Schack [24] points out, a physical realization of a quantum baker's map.

### III. INTEGRATED OPTICS APPROACH

A linear optical simulation of the quantum baker's map may be developed from a different approach. This approach may offer a more tractable means of implementation. It is always possible to build an  $N \times N$  symmetric multiport device [25] which performs the DFT. The simplest realization of such a device is a symmetric  $N \times N$  fiber coupler [26]. In a single coupler an  $N$ -dimensional DFT is performed.

The inverse DFT for an  $N \times N$  multiport device requires two unitary operations. For any unitary matrix  $U$ ,  $U^{-1} = U^\dagger$ . Hence,  $U_{ij}^{-1} = U_{ji}^*$ . Thus, the inverse DFT is given by

$$(F_N)_{nm}^{-1} = \frac{1}{\sqrt{N}} e^{-2\pi i mn/N}. \quad (3.1)$$

The inverse DFT can be obtained from a symmetric multiport device by a simple relabeling of paths. We introduce an unitary operation  $T$  defined by

$$(F_N)^{-1} = T(F_N) \quad (3.2)$$

where for three bits  $T$ , in matrix form, is given by

$$T = \begin{pmatrix} 1 & 0 & 0 & 0 & 0 & 0 & 0 & 0 \\ 0 & 0 & 0 & 0 & 0 & 0 & 0 & 1 \\ 0 & 0 & 0 & 0 & 0 & 0 & 1 & 0 \\ 0 & 0 & 0 & 0 & 0 & 1 & 0 & 0 \\ 0 & 0 & 0 & 0 & 1 & 0 & 0 & 0 \\ 0 & 0 & 0 & 1 & 0 & 0 & 0 & 0 \\ 0 & 0 & 1 & 0 & 0 & 0 & 0 & 0 \\ 0 & 1 & 0 & 0 & 0 & 0 & 0 & 0 \end{pmatrix}. \quad (3.3)$$

The  $T$  matrix simply swaps rows of the DFT. For example, the 111 path is relabeled as the 001 path. Hence, the quantum Baker's map transformation can be rewritten as

$$B = T(F_N) \begin{pmatrix} F_{N/2} & 0 \\ 0 & F_{N/2} \end{pmatrix}. \quad (3.4)$$

One can consider the QBM as simply a rotation operation

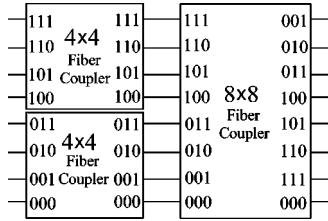


FIG. 2. Optical realization of a 3-bit quantum baker’s map using multiport devices (e.g., a symmetric  $N \times N$  fiber coupler) to generate the DFT and inverse DFT. Only three optical elements are needed to implement the map.

on some vector in the Hilbert space. The quantum analogy of the classical trajectory is looking at the evolution of the direction of the vector. Hence, varying the input state or perturbing the map by introducing phase or amplitude shifts will result in various phase and amplitude outputs out of the  $8 \times 8$  coupler.

The optical realization of the map is shown in Fig. 2. The first operation groups the paths by the most significant bit. All of the paths having a most significant bit value of 1 (0) enter the input ports of the top (bottom) symmetric  $4 \times 4$  device (boxes are shown to represent the couplers for visual clarity). The output fibers of the  $4 \times 4$  couplers are taken to the inputs of the  $8 \times 8$  coupler. The  $T$  operation is realized by appropriately labeling the outputs of the  $8 \times 8$  coupler. Thus, Fig. 2 represents one iteration of the quantum baker’s map. As can be seen it was obtained with only three optical devices.

IV. DISCUSSION

Let us examine various input states in terms of single-photon interferometry. The simplest input state is to have a photon enter only a single input port. We will use this case and the analogous classical field (only intensity in a single input port) in the examples below. On the other hand, the photon can be put into a superposition of various input paths. For example, equal amplitudes in each of the inputs can be realized by introducing another amplitude splitting device. The simplest realization of this device is to have another  $8 \times 8$  fiber coupler. By coupling the photon into one of the paths of the input coupler, the photon will have an equal probability of being in each path. If the photon is coupled into the 000 path and all of the pathlengths between the input coupler and the QBM are the same, then the input state is given by  $1/\sqrt{8}(|000\rangle + |001\rangle + \dots + |111\rangle)$ .

After some iteration of the map the output must be measured. The measurement, in the case of single photons, will collapse the wave function so that the photon will be in only one of the output paths. The output path in which the photon is found can vary strongly from iteration to iteration. For a fixed map the probabilities of finding the photon in a particular output ports is fixed. However, perturbations of the map lead to strong variations in the probabilities. This is perhaps easiest to visualize for a classical field which corresponds to an ensemble of these individual realizations. We are assuming weak classical fields in which photons only interfere with themselves.

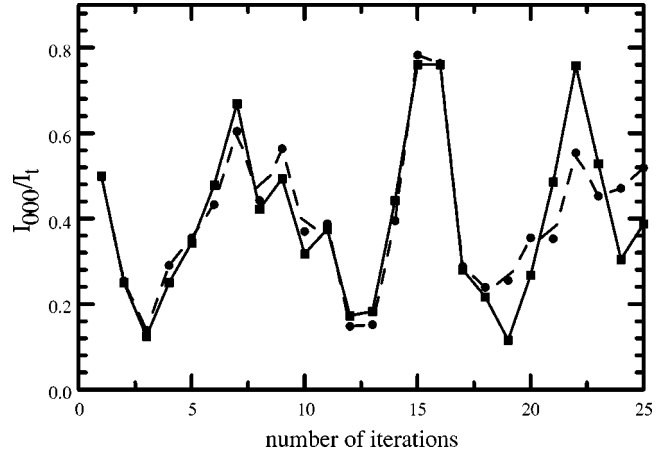


FIG. 3. Relative intensity out of the 000 path vs the number of iterations of the map. All of the light is initially coupled into the 000 path. The squares connected by the solid lines are for the output of the unperturbed quantum baker’s map. The output of the perturbed map (circles connected by the dashed line) was generated by adding a  $2\pi/100$  phase shift in the 000 path between the  $4 \times 4$  and  $8 \times 8$  couplers.

Assume that the total input intensity is given by  $I_t$  and the measured intensity coming out of the 000 output of the  $8 \times 8$  coupler is  $I_{000}$ . The intensity ratio  $I_{000}/I_t$  is equal to the probability that the photon will be measured in the 000 path. For example, in Fig. 3 all of the input light is coupled into the 000 input. The dots connected by the solid line represent the intensity ratio  $I_{000}/I_t$  out of the 000 path of the  $8 \times 8$  coupler as a function of the number of iterations of the map (similar intensity plots could be obtained for each of the outputs of the coupler). The intensity ratio from each output path for the  $i$ th iteration is equal to the probability that a photon would be measured in that path if one decides to measure the photon after  $i$  iterations of the map. The probability of finding the photon in the 000 path can vary strongly from iteration to iteration and it does not converge to any particular value after many iterations of the map.

One clear limitation of this approach is the size of the  $N \times N$  coupler. At this time,  $8 \times 8$  couplers are readily available commercially. A few others points should be addressed about the implementation of such a device. These couplers and other integrated optics are not perfect. They have inequalities in the splittings, absorption, phase shifts, etc. Thus the construction of the exact QBM is difficult. This is particularly true since the map is very sensitive to perturbation. Hence, these phase shifts and unequal amplitude splittings at the couplers cause significant deviations from the desired map. For example, consider what happens to the QBM when a phase shift of  $2\pi/100$  is introduced between the output of the  $4 \times 4$  coupler and the input of the  $8 \times 8$  coupler along the 000 path only. This can be represented by a diagonal matrix with all of the elements equal to 1 except the upper-left-most matrix element which has a value of  $e^{i2\pi/100}$ . Figure 3 shows two intensity versus iteration plots. The unperturbed situation is shown with a solid line joining the points. The perturbed situation is shown with a dashed



line joining the points. One can notice that the intensity difference between the perturbed and unperturbed situation after 18 iterations becomes quite significant. Similar plots can be obtained for each of the eight outputs. However, the 000 path output is the most sensitive to phase changes in its path. In addition, there will always be some error introduced due to unequal amplitude splittings at each of the fiber couplers. For example, in Fig. 2 it was assumed that if light entered one of the input ports of the  $4 \times 4$  couplers that 25% of the light would leave in each of the output ports. However, experimentally this is not possible since imperfections in the couplers will always exist.

Spurious phase shifts and unequal amplitude splittings are perturbations from the originally proposed QBM. However, it is precisely the hypersensitivity of the map due to perturbation that is of interest. This suggests that if a particular map is realized that is an approximation of the QBM designed above, this would retain the interesting physics. That is, the characteristic behavior of a particular set up can be obtained and then perturbations from this map be studied.

Multiple iterations of this QBM can be obtained by building consecutive circuits each one appearing as in Fig. 2. For a small number of iterations, this is probably the preferred

method. It should also be possible to obtain multiple iterations of the QBM by rerouting the output to the input of the device. Either means has significant technical challenges. The coherence must be preserved from iteration to iteration. Care must be taken to not measure the output until the desired iteration is reached. Of course nonunitary operations such as absorption in the optical devices is a serious concern.

This paper has shown how linear optics can be used to simulate or realize the quantum baker's map. Building such quantum analogs using single photons is rather instructive, since the trajectory of the photon represents the evolution of the state. These ideas can be carried over to the implementation of an exhaustive search [3,4,17]. In that case, one can observe the various paths from an initial state to some final state by following the trajectories of the photon. The actual physical realization of such linear optical analogs or simulations should provide further insight into the studies of quantum networks.

#### ACKNOWLEDGMENT

This work was supported by the National Science Foundation under Grant No. PHY-9733643.

- 
- [1] P. W. Shor, in *Proceedings of the 35th Symposium on Foundations of Computer Science*, edited by S. Goldwasser (IEEE, Los Alamitos, CA, 1994), pp. 124-134.
  - [2] A. Ekert and R. Jozsa, *Rev. Mod. Phys.* **68**, 733 (1996).
  - [3] T. Hogg, *Phys. Rev. Lett.* **80**, 2473 (1998).
  - [4] L. K. Grover, *Phys. Rev. Lett.* **80**, 4329 (1998).
  - [5] R. P. Feynmann, *Found. Phys.* **16**, 507-531 (1986).
  - [6] J. I. Cirac and P. Zoller, *Phys. Rev. Lett.* **74**, 4091 (1995); A. Steane, *Appl. Phys. B: Laser Optics* **64**, 623-642 (1997); C. Monroe, D. M. Meekhof, B. E. King, W. M. Itano, and D. J. Wineland, *Phys. Rev. Lett.* **75**, 4714 (1995).
  - [7] D. G. Cory, M. P. Price, and T. F. Havel, *Physica D* **120**, 82 (1998).
  - [8] D. G. Cory, M. D. Price, W. Maas, E. Knill, R. Laflamme, W. H. Zurek, T. F. Havel, and S. S. Somaroo, *Phys. Rev. Lett.* **81**, 2152 (1998).
  - [9] Q. A. Turchette, C. J. Hood, W. Lange, H. Mabuchi, and H. J. Kimble, *Phys. Rev. Lett.* **75**, 4710 (1995).
  - [10] G. K. Brennen, C. M. Caves, Poul S. Jessen, and I. H. Deutsch, *Phys. Rev. Lett.* **82**, 1060 (1999).
  - [11] D. Loss and D. P. DiVincenzo, *Phys. Rev. A* **57**, 120 (1998).
  - [12] N. J. Cerf, C. Adami, and P. G. Kwiat, *Phys. Rev. A* **57**, R1477 (1998).
  - [13] S. Takeuchi, in *Proceedings of the 4th Workshop on Physics and Computation (PhysComp96)*, edited by T. Toffoli, M. Bifare, and J. Leao (New England Complex Systems Institute, Boston, 1996), p. 299.
  - [14] J. F. Clauser and J. P. Dowling, *Phys. Rev. A* **53**, 4587 (1996).
  - [15] J. Summhammer, *Phys. Rev. A* **56**, 4324 (1997).
  - [16] R. J. C. Spreeuw, *Found. Phys.* **28**, 361 (1998).
  - [17] P. G. Kwiat, J. R. Mitchell, P. D. D. Schwindt, and A. G. White, LANL xxx-archive quant-ph/9905086.
  - [18] C. H. Bennett, G. Brassard, C. Crepeau, R. Jozsa, A. Peres, and W. K. Wootters, *Phys. Rev. Lett.* **70**, 1895 (1993).
  - [19] I. L. Chuang and Y. Yamamoto, *Phys. Rev. A* **52**, 3489 (1995); *Phys. Rev. Lett.* **76**, 4281 (1996).
  - [20] T. Sleator and H. Weinfurter, *Phys. Rev. Lett.* **74**, 4087 (1995).
  - [21] H. F. Chau and F. Wilczek, *Phys. Rev. Lett.* **75**, 748 (1995).
  - [22] A. Barenco, C. H. Bennett, R. Cleve, D. P. DiVincenzo, N. Margolus, P. Shor, T. Sleator, J. A. Smolin, and H. Weinfurter, *Phys. Rev. A* **52**, 3457 (1995).
  - [23] For example, a 3-path-bit Toffoli gate can be constructed by crossing the 111 and 110 paths and then relabeling the paths. A 3-path-bit Fredkin gate can be constructed by crossing the 110 and 101 paths and relabeling the paths. Any phase gate can be realized by placing phase shifters in the appropriate paths. In a 2-path and 1-polarization bit scheme, a Deutsch gate can be realized by placing a polarization rotator in the 11 path. Other combinations of the Toffoli and Fredkin gates exist and all of them only require a single unitary operation.
  - [24] R. Schack, *Phys. Rev. A* **57**, 1634 (1998).
  - [25] M. Zukowski, A. Zeilinger, and M. A. Horne, *Phys. Rev. A* **55**, 2564 (1997).
  - [26] G. Weihs, M. Reck, H. Weinfurter, and A. Zeilinger, *Opt. Lett.* **21**, 302 (1996).
  - [27] A possible conclusion is that these ideas could be used to factor large numbers. However, in order to factor a number approximately 60 digits in length would require two dimensions of the known universe to be filled with single-mode fibers.
  - [28] M. Reck, A. Zeilinger, H. J. Bernstein, and P. Bertani, *Phys. Rev. Lett.* **73**, 58 (1994).

- [29] Large area avalanche photodiodes are up to 90% efficient in detecting single photons in the visible and near IR.
- [30] C. K. Law and J. H. Eberly, Phys. Rev. Lett. **76**, 1055 (1996); C. J. Hood, M. S. Chapman, T. W. Lynn, and H. J. Kimble, *ibid.* **80**, 4157 (1998).
- [31] N. L. Balazs and A. Voros, Ann. Phys. (N.Y.) **190**, 1 (1989).
- [32] R. Schack and C. M. Caves, Phys. Rev. Lett. **71**, 525 (1993).
- [33] J. H. Hannay, J. P. Keating, and A. M. Ozorio de Almeida, Nonlinearity **7**, 1327 (1994).